

EXPERIMENTAL INVESTIGATION ON MECHANICAL PROPERTIES OF GRADE 1670 STEEL WIRES UNDER AND AFTER ELEVATED TEMPERATURE

Er-Feng Du ^{1,*}, Xiao-Bo Hu ², Zhong Zhou ², Qian Li ², Xiao Lyu ³ and Yi-Qun Tang ²

¹ China-Pakistan Belt and Road Joint Laboratory on Smart Disaster Prevention of Major Infrastructures, Southeast University, Nanjing, China

² School of Civil Engineering, Southeast University, Nanjing, China

³ School of Civil Engineering, Shandong Jianzhu University, Ji'nan, China

* (Corresponding author: E-mail: erfengdu@seu.edu.cn)

ABSTRACT

Grade 1670 steel wires were selected for elevated-temperature and post-elevated-temperature tensile tests. The test data were analyzed through comparison with the results in existing literatures. The elevated-temperature test results indicate that, mechanical properties of the steel wires degraded with the increase of temperature. The mechanical behaviors of the steel wires degraded rapidly at the temperature exceeding 300°C, and the load-carrying ability was substantially lost when the temperature increased up to 700°C. In the post-elevated-temperature test, the modulus of the steel wire was almost completely recovered after cooling from the elevated temperatures. The nominal yield strength and ultimate strength degraded obviously after cooling from the temperature exceeding 400°C. Based on the test data, the reduction factors of the mechanical properties at and after elevated temperatures are fitted as a function of the temperature, and constitutive models of the steel wires are established. The results can provide technical supports for the analysis of fire performance of prestressed cable support structures, and their post-fire repair.

ARTICLE HISTORY

Received: 20 July 2022
Revised: 22 August 2022
Accepted: 10 January 2023

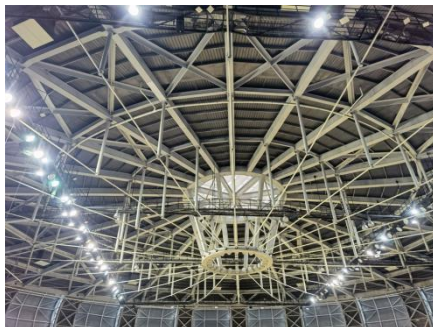
KEYWORDS

Steel wires;
Elevated temperatures;
Mechanical properties;
Experimental research;
Stress-strain curve

Copyright © 2023 by The Hong Kong Institute of Steel Construction. All rights reserved.

1. Introduction

Steel cables are the key members of long-span prestressed steel structures such as cable domes, string domes and tension beams, as shown in Fig. 1. However, mechanical properties of the steel cables are significantly degraded at elevated temperatures, thereby seriously influencing the safety of the overall structure. The steel cable is mainly composed of steel wires, and thus the study on the elevated-temperature and post-elevated-temperature mechanical properties, such as the elastic modulus, proportional limit, yield strength, and ultimate strength of the steel wire, is of great significance to the fire resistance analysis and post-fire evaluation of large-span prestressed steel structures.



(a) String dome structure



(b) Tension beam structure

Fig. 1 Long-span prestressed steel structures

Mechanical properties of steel cables at elevated temperatures have been investigated by scholars. Zhou et al.[1] tested mechanical behaviors of 27 Grade 1860 prestressed steel cables from ambient temperatures to 700°C, and obtained stress-strain curves of the steel cables at different temperatures. Zong et al.[2,3] conducted experimental research on mechanical performances of Grade 1860 prestressed steel cables at elevated temperatures, and obtained the degradation law and mechanical model of the steel cables. Fontanari et al.[4] studied mechanical properties of C80 high-carbon steel cables at elevated temperatures, and provided a numerical analysis method to study the fire resistance of steel cables. Conor et al.[5] performed tensile tests on ASTM A416-12a steel cables composed of 7 steel wires at elevated temperatures, and as compared with Eurocodes, the results showed that the Eurocodes cannot accurately predict the stress-strain relationship of the steel cable. Shakya et al.[6] studied the mechanical performance of steel cables composed of 7 Grade 1860 steel wires at elevated temperatures, and gave an empirical equation for the mechanical properties of steel cables as a function of the temperature. Du et al.[7-10] carried out tensile tests at elevated temperatures on a Grade 1670 steel cable, a Grade 1670 parallel steel wire strand, and a Grade 1860 steel cable, and revealed the relationship between the reduction factor of mechanical behaviors and the temperature. Sun et al. [11-13] conducted tensile tests at elevated temperatures on a Grade 1500 stainless steel cable, a Grade 1670 high-vanadium cable, and a Grade 1770 steel wire coated with 5% zinc-aluminum alloy, and obtained a reduction factor equation for mechanical properties of steel cables and steel wires.

In view of the mechanical properties of steel cables after exposure to elevated temperatures, Fan et al.[14] studied the mechanical properties of Grade 1570 high-strength prestressed steel wires after cooling to ambient temperature from elevated temperatures, and obtained variation laws of mechanical behaviors of steel wires. Lu et al.[15,16] tested the post-fire mechanical performances of a Grade 1670 steel cable and prestressed steel wires of different grades, and investigated effects of different cooling methods on the mechanical behaviors of steel cables and steel wires. Zheng et al.[17] and Atienza et al.[18] performed tensile tests on Grade 1770 prestressed steel wires after cooling from elevated temperatures, and obtained the degradation law of mechanical properties of steel wires after high temperature. Zong et al.[19] conducted experimental research on a Grade 1860 prestressed steel cable after heating, and revealed the relationship between the mechanical properties of the steel cable and the exposure temperature. Zhang et al.[20] carried out experimental research on the post-fire mechanical properties of a Grade 1670 cold-drawn steel wire used in suspension bridges, and analyzed the influence of the exposure temperature on the mechanical behaviors of the steel wire after cooling.

Though aforementioned scholars have performed a series of studies on the

mechanical performance of steel wires, and accumulated a lot of test data, due to the continuous improvement in performance of steel wires, mechanical behaviors of the newly emerging steel cables in engineering are less investigated. Therefore, this paper conducts an experimental study on elevated-temperature and post-elevated-temperature mechanical properties of Grade 1670 prestressed steel wires, and provides a reference for the property evaluation of prestressed steel structures under and after fire.

2. Test program

2.1. Test equipment

The test equipment for elevated-temperature and post-elevated-temperature mechanical properties of steel wires is shown in Fig. 2. The loading device was an electronic universal testing machine, with a maximum tensile force of 300kN. The specimen was heated by an electronic elevated-temperature furnace. The furnace was equipped with multi-layer resistance wires. The furnace had a diameter of 24cm and a height of 46cm. The maximum temperature in the furnace could reach 1200°C. The strain of the steel wire was measured by an elevated-temperature strain extensometer with a gauge length of 50mm. During the measurement, the knife edge at the end of the extensometer was closely contacting the specimen. Data such as the strain and temperature were automatically collected by a computer.

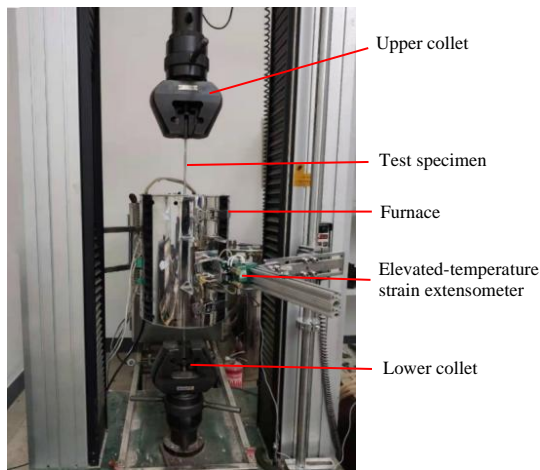


Fig. 2 Electronic universal testing machine

2.2. Test specimens

The steel wires used in the elevated-temperature and post-elevated-temperature tests had a strength grade of 1670MPa, a diameter of 7mm, and a length of 80cm. Due to the high strength and hardness of the prestressed steel wire, it is easy for the wire to slip when directly clamped by the testing machine. Therefore, pier heads and clip anchors were set at both ends of the specimen for effective clamping. The clamping device is shown in Fig. 3. The diameter of the pier head was 14mm, and the diameter and length of the clip anchor were 25mm and 80mm, respectively. A length of 15cm at the upper and lower ends of the steel wire outside the elevated-temperature furnace was set aside to cool in the air, so as to avoid the influence of high temperatures on the collets of the testing machine.

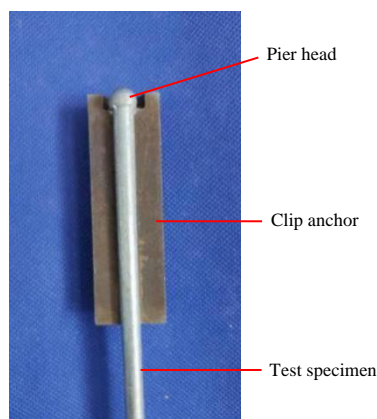


Fig. 3 Clamping device for specimen

2.3. Loading procedure

8 temperature levels were set for the tests of elevated-temperature mechanical properties, including 20°C (ambient temperature), 100°C, 200°C, 300°C, 400°C, 500°C, 600°C, and 700°C, respectively. Tests were conducted according to the test methods specified in “Metallic materials - Tensile testing - Part 1: Method of test at room temperature” (GB/T228.1-2010)[21] and “Metallic materials - Tensile testing - Part 2: Method of test at elevated temperature” (GB/T228.2-2015)[22]. The specimens were heated to a specified temperature and then kept for 30 min, to ensure the temperature evenly distributed in the specimens. During the heating and isothermal processes, no tension was applied on the test specimen. Stretching was performed after the temperature distributed uniformly and stably, at a constant rate of 3 mm/min.

5 temperature levels were set for the tests of post-elevated-temperature mechanical properties, including 300°C, 400°C, 500°C, 600°C, and 700°C, respectively. According to the same heating method as that in the elevated-temperature test, the specimens were firstly heated to the target temperature, subsequently kept constant at that temperature for 30 min, and then naturally cooled to ambient temperature followed by stretching. The stretching method was the same as that in the elevated-temperature test.

3. Results and analysis of the elevated-temperature test

3.1. Visual observations

Apparent characteristics of the specimens after the elevated-temperature tensile test are shown in Fig. 4. The heating temperatures of various specimens from left to right were 20°C, 100°C, 200°C, 300°C, 400°C, 500°C, 600°C and 700°C, respectively. At 20°C (ambient temperature), the specimen broke near the pier head, due to the damage at the pier head caused during cold rolling. While at other temperatures, the specimens broke in the heated area. At 20°C, the specimen was damaged at an oblique angle of 45°. At 200°C ~ 400°C, the metallic luster of the specimen became darker, and the fracture was cup-shaped with serrations. At 500°C, the metallic luster on the surface of the specimen completely faded, and the fracture began to be tapered. At 600°C, the specimen was light yellow, and the fracture was more tapered. When the temperature was 700°C, the specimen was yellowish brown.

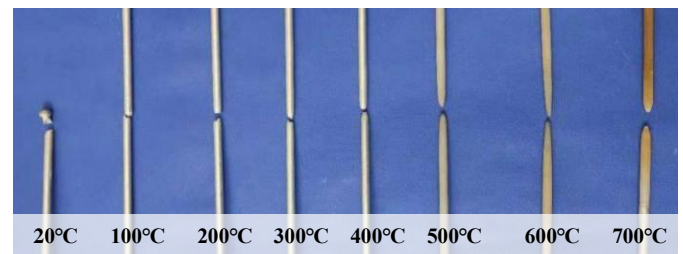


Fig. 4 Failure modes of steel wires after elevated-temperature test

3.2. Analysis of test results

According to the strain data obtained in the test, stress-strain curves of the specimens at different temperatures are plotted in Fig. 5. At the same time, reduction factors of mechanical properties of the steel wires under various

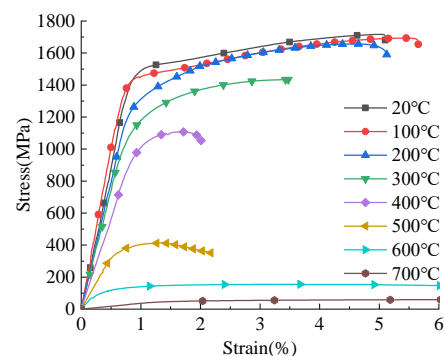


Fig. 5 Stress-strain curves of steel wires at elevated temperatures

temperatures can be calculated, as shown in Table 1. It can be seen from the

figure and the table that, with the increase of temperature, the mechanical properties such as the elastic modulus, nominal yield strength (i.e., the yield strength corresponding to the strain level of 0.2%), and ultimate strength of the specimens all degraded. The elastic modulus of the specimen remained unchanged at 100°C, and decreased at 200°C to 89% of that at ambient temperature. Above 300°C, the rate of decrease of the elastic modulus was accelerated with the temperature increase. At 500°C, the elastic modulus was

37% of that at ambient temperature, and the elastic modulus at 700°C was only 2% of that at room temperature. As the temperature increased, the nominal yield strength and ultimate strength of the specimens decreased slowly below 200°C, within a range of 10%, and decreased rapidly above 400°C. At 500°C, the nominal yield strength and the ultimate strength decreased by 74% and 76%, respectively. At 700°C, the nominal yield strength and ultimate strength were less than 10% of those at ambient temperature.

Table 1

Mechanical properties of steel wires at elevated temperatures

T (°C)	$E_s(T)$ (GPa)	$E_s(T)/E_s$	$\sigma_{0.2}(T)$ (MPa)	$\sigma_{0.2}(T)/\sigma_{0.2}$	$\sigma_b(T)$ (MPa)	$\sigma_b(T)/\sigma_b$
20	180	1.00	1500	1.00	1703	1.00
100	180	1.00	1449	0.97	1693	0.99
200	160	0.89	1295	0.86	1656	0.97
300	148	0.82	1180	0.79	1434	0.84
400	115	0.64	1010	0.67	1108	0.65
500	66	0.37	383	0.26	414	0.24
600	31	0.17	123	0.08	155	0.09
700	3.5	0.02	40	0.04	47	0.03

Notes: T is the temperature; $E_s(T)$ and E_s are the elastic modulus of steel wires at temperature T and ambient temperature, respectively; $\sigma_b(T)$ and σ_b are the ultimate strength of steel wires at temperature T and ambient temperature, respectively; $\sigma_{0.2}(T)$ and $\sigma_{0.2}$ are the yield strength of steel wires at temperature T and ambient temperature, respectively.

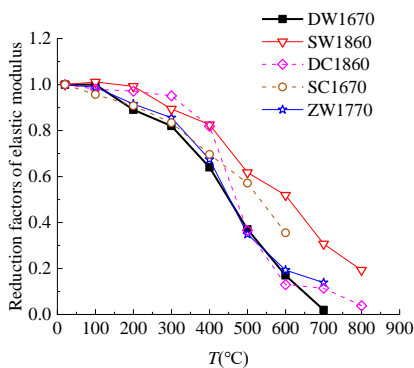
In general, the mechanical performances of the prestressed steel wires changed little with the temperature below 300°C and degraded significantly at 300°C ~ 600°C, and the load-carrying ability was substantially lost when the temperature reached 700°C.

3.3. Comparison and discussion

Reduction factors of the elastic modulus, nominal yield strength and ultimate strength obtained by test results of this paper are compared with those of a Grade 1860 prestressed steel wire of Shakya et al. [6], a Grade 1770 prestressed steel wire of Zheng et al. [16], a Grade 1860 steel cable of Du et al. [7], and a Grade 1670 high-vanadium cable of Sun et al. [12], as shown in Figures 6 ~ 8. In the figures, the reduction factors in this paper, Shakya et al. [6], Zheng et al. [16], Du et al. [7] and Sun et al. [12] are marked with DW1670, SW1860, ZW1770, DC1860 and SC1670, respectively.

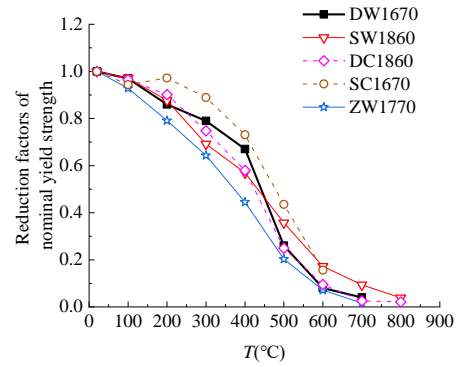
(1) Comparison of reduction factors of elastic modulus

As shown in Fig. 6, in terms of the steel wires, the reduction factors of elastic modulus obtained by test results of this paper (DW1670) and ZW1770 are generally lower than SW1860, and except for 700°C, the test results of this paper are very close to ZW1770. As compared with the test results of steel cables, DW1670 is close to DC1860 at 100°C, 500°C and 600°C, and lower than DC1860 at other temperatures. DW1670 is close to SC1670 below 400°C, and lower than SC1670 when the temperature is above 500°C.

**Fig. 6** Comparison of reduction factors of elastic modulus

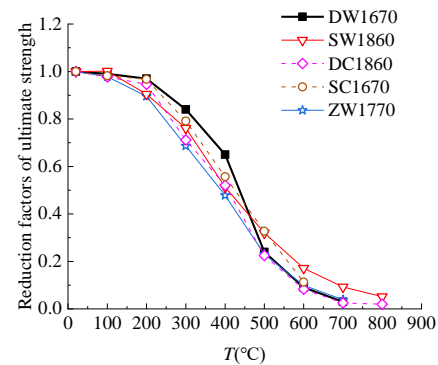
(2) Comparison of reduction factors of nominal yield strength

As can be seen in Fig. 7, DW1670 and SW1860 are generally higher than ZW1770. DW1670 is close to SW1860 below 200°C, higher than SW1860 at 300°C and 400°C, and lower than SW1860 above 500°C; close to DC1860 except for 400°C at which DW1670 is higher than DC1860. The reduction factors of this paper (DW1670) are lower than SC1670 except for 100°C at which DW1670 is close to SC1670.

**Fig. 7** Comparison of reduction factors of nominal yield strength

(3) Comparison of reduction factors of ultimate strength

As exhibited in Fig. 8, the reduction factors of ultimate strength obtained by test results of this paper (DW1670) are higher than SW1860 and ZW1770 from 200°C to 400°C, and close to ZW1770 but lower than SW1860 above 500°C. DW1670 is higher than SC1670 and DC1860 at 300°C and 400°C, and close to SC1670 and DC1860 from 500°C to 700°C except for 500°C at which DW1670 is lower than SC1670.

**Fig. 8** Comparison of reduction factors of ultimate strength

In general, though the reduction factors of mechanical properties of prestressed steel wires and cables of different strength grades are discrete to a certain extent, their variation laws are basically the same. The mechanical properties of steel cables under elevated temperature can be approximately represented by those of steel wires.

3.4. Fitting equation for reduction factors

According to the test data, fitting equations for reduction factors of mechanical properties of steel wires at high temperatures are obtained as follows,

3.4.1. Elastic modulus

$$\frac{E_s(T)}{E_s} = \frac{1}{1 + e^{0.0101(T-550)}} \quad (1)$$

where, $E_s(T)$ and E_s are the elastic modulus of steel wires at temperature T and ambient temperature, respectively.

Fig. 9 gives the fitting curve of Eq. (1).

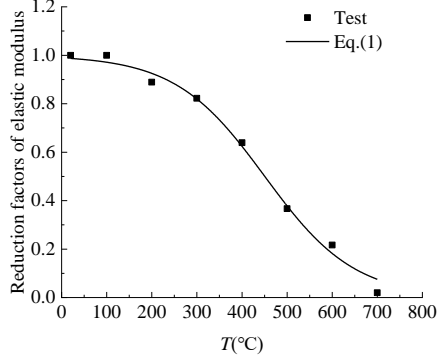


Fig. 9 Reduction factor of elastic modulus-temperature curve

3.4.2. Proportional limit

$$\frac{\sigma_p(T)}{\sigma_p} = 7.46 \times 10^{-3} T^3 - 8.94 \times 10^{-5} T^2 + 1.23 \times 10^{-3} T + 0.97 \quad (2)$$

where, $\sigma_p(T)$ and σ_p are the proportional limit of steel wires at temperature T and ambient temperature, respectively.

The fitting curve of Eq. (2) is plotted in Fig. 10.

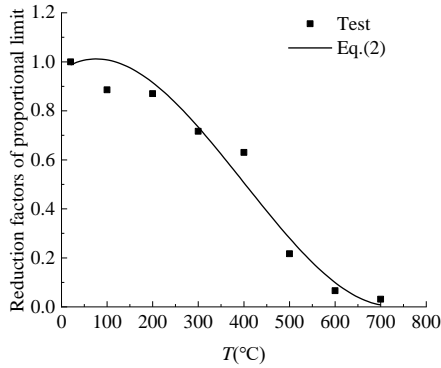


Fig. 10 Reduction factor of proportional limit-temperature curve

3.4.3. Ultimate strength

$$\frac{\sigma_b(T)}{\sigma_b} = \frac{1}{1 + e^{0.0147(T-432)}} \quad (3)$$

where, $\sigma_b(T)$ and σ_b are the ultimate strength of steel wires at temperature T and ambient temperature, respectively.

Fig. 11 shows the fitting curve of Eq. (3).

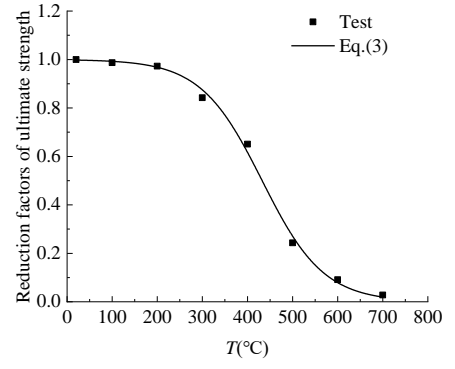


Fig. 11 Reduction factor of ultimate strength-temperature curve

3.4.4. Strain at ultimate strength

The strain corresponding to the maximum stress of the specimen reaching the ultimate strength is the strain at ultimate strength. The reduction factor of the strain at ultimate strength at elevated temperature is obtained as follows,

$$\frac{\varepsilon_b(T)}{\varepsilon_b} = \begin{cases} 1 & 20^\circ\text{C} \leq T \leq 180^\circ\text{C} \\ -3.30 \times 10^{-3} T + 1.57 & 180^\circ\text{C} \leq T \leq 400^\circ\text{C} \\ 3.40 \times 10^{-4} T + 9.67 \times 10^{-2} & 400^\circ\text{C} \leq T \leq 500^\circ\text{C} \\ 5.80 \times 10^{-3} T - 2.62 & 500^\circ\text{C} \leq T \leq 700^\circ\text{C} \end{cases} \quad (4)$$

where, $\varepsilon_b(T)$ and ε_b are the strain at ultimate strength of steel wires at temperature T and ambient temperature, respectively.

The fitting curve of Eq. (4) is shown in Fig. 12.

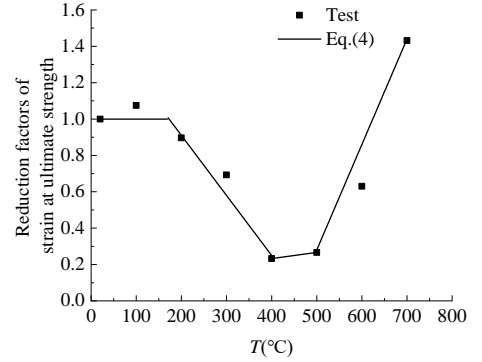


Fig. 12 Reduction factor of strain at ultimate strength-temperature curve

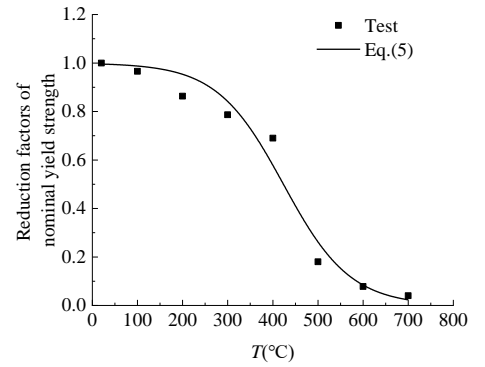


Fig. 13 Reduction factor of nominal yield strength-temperature curve

3.4.5. Nominal yield strength

$$\frac{\sigma_{0.2}(T)}{\sigma_{0.2}} = \frac{1}{1 + e^{0.0135(T-424)}} \quad (5)$$

where, $\sigma_{0.2}(T)$ and $\sigma_{0.2}$ are nominal yield strength of steel wires at temperature T and ambient temperature, respectively.

The fitting curve of Eq. (5) is shown in Fig. 13.

3.4.6. Strain at nominal yield strength

$$\frac{\varepsilon_{0.2}(T)}{\varepsilon_{0.2}} = \begin{cases} 1 & 20^\circ\text{C} \leq T \leq 380^\circ\text{C} \\ -2.40 \times 10^{-3}T + 1.9161 & 380^\circ\text{C} \leq T \leq 600^\circ\text{C} \end{cases} \quad (6)$$

where, $\varepsilon_{0.2}(T)$ and $\varepsilon_{0.2}$ are strain at nominal yield strength of steel wires at temperature T and ambient temperature, respectively.

The fitting curve of Eq. (6) is presented in Fig. 14.

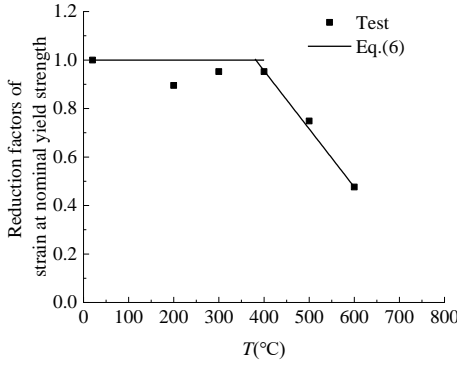


Fig. 14 Reduction factor of strain at nominal yield strength-temperature curve

3.5. Constitutive equation

The constitutive equation of the steel wires at elevated temperatures is fitted with a trilinear line. The trilinear line includes a segment from the origin to the proportional limit point, a segment from the proportional limit point to the nominal yield strength point, and a segment from the nominal yield strength point to the ultimate strength point. The fitting equation is shown as follows,

$$\sigma = \begin{cases} E_s(T) \times \varepsilon & 0 \leq \varepsilon \leq \frac{\sigma_p(T)}{E_s(T)} \\ \frac{\sigma_{0.2}(T) - \sigma_p(T)}{\varepsilon_{0.2}(T) - \frac{\sigma_p(T)}{E_s(T)}} \times \left[\varepsilon - \frac{\sigma_p(T)}{E_s(T)} \right] + \sigma_p(T) & \frac{\sigma_p(T)}{E_s(T)} \leq \varepsilon \leq \varepsilon_{0.2}(T) \\ \frac{\sigma_b(T) - \sigma_{0.2}(T)}{\varepsilon_b(T) - \varepsilon_{0.2}(T)} \times [\varepsilon - \varepsilon_{0.2}(T)] + \sigma_{0.2}(T) & \varepsilon_{0.2}(T) \leq \varepsilon \leq \varepsilon_b(T) \end{cases} \quad (7)$$

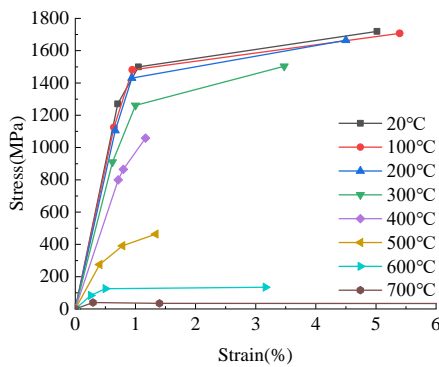


Fig. 15 Stress-strain fitting curves of steel wires at elevated temperatures

Stress-strain curves at various temperatures obtained by the equation are shown in Fig. 15.

4. Results and analysis of post-elevated-temperature test

4.1. Visual observations

Fig. 16 shows the failure modes of the specimens after the tensile test. The maximum temperatures experienced by various specimens from left to right were 300°C, 400°C, 500°C, 600°C and 700°C, respectively. When the specimen was experiencing a temperature of 300°C, it was broken near the pier head, with a fracture along the 45° direction, which phenomenon was the same as the specimen broken at ambient temperature. The specimens that had been exposed to a temperature above 400°C were all broken in the heated area after cooling, and their fractures were all tapered and necked. After exposure to 500°C, the metallic luster on the surface of the specimen faded. The surface of the specimen turned light yellow after exposure to 600°C, and yellowish-brown after exposure to 700°C.

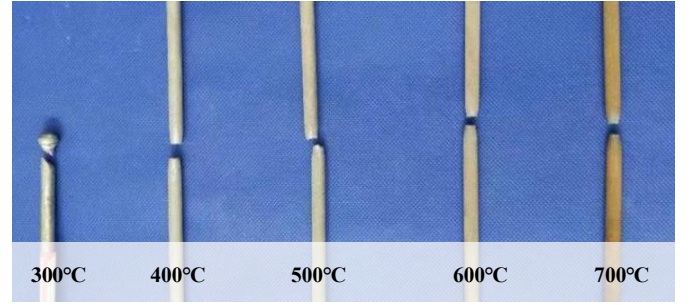


Fig. 16 Failure modes of steel wires after post-elevated-temperature test

4.2. Analysis of test results

Stress-strain curves of the specimens cooled from different temperatures are presented in Fig. 17. According to the test data, reduction factors of mechanical properties of the steel wires after exposure to elevated temperatures can be obtained, as tabulated in Table 2. It can be found from the figure and table that, the elastic modulus of the specimens did not change obviously after cooling from the elevated temperatures, and their reduction factors were all within 10%. Therefore, the specimens could recover the initial elastic modulus after fire. After cooling from the temperature below 400°C, the nominal yield strength and ultimate strength of the specimens had no evident degradation, and the reduction factor was within 10%. The nominal yield strength and ultimate strength of the specimens began to degrade significantly after cooling from the temperature above 400°C. The nominal yield strength decreased by 22% and the ultimate strength decreased by 23% after exposure to 500°C. With the increase of the maximum exposure temperature, the degradation of the nominal yield strength and ultimate strength of the specimen became more obvious. After cooling from the temperature up to 700°C, the nominal yield strength and the ultimate strength had decreased to 32% and 40% of that at the ambient temperature, respectively.

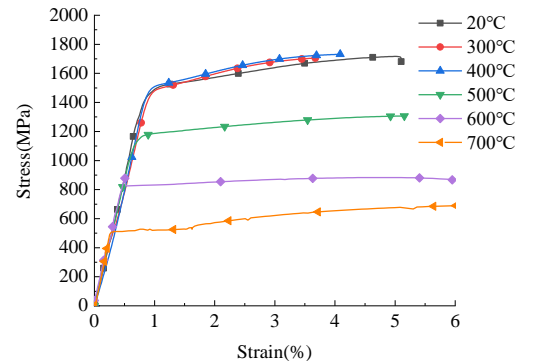


Fig. 17 Stress-strain curves of steel wires after cooling from elevated temperatures

4.3. Comparison and discussion

Since the elastic modulus of the steel wires changed very little after cooling from elevated temperatures, only the reduction factors of the nominal yield strength and ultimate strength of the steel wires are compared. Reduction factors of the nominal yield strength and ultimate strength obtained in this

paper are compared with those of a Grade 1570 prestressed steel wire of Fan *et al.* [14], a Grade 1670 galvanized prestressed steel wire of Lu *et al.* [15], and a Grade 1770 prestressed steel wire of Zheng *et al.* [17] and Atienza *et al.* [18], as exhibited in Figures 18 and 19. In the figures, the reduction factors in this paper, Fan *et al.* [14], Lu *et al.* [15], Zheng *et al.* [17] and Atienza *et al.* [18] are marked with DW1670, FW1570, LW1670, ZW1770 and AW1770, respectively.

(1) Comparison of nominal yield strength

Table 2

Mechanical properties of steel wires after cooling from elevated temperatures

$T(^{\circ}\text{C})$	$E_s^{\#}(T)(\text{GPa})$	$E_s^{\#}(T)/E_s$	$\sigma_{0.2}^{\#}(T)(\text{MPa})$	$\sigma_{0.2}^{\#}(T)/\sigma_{0.2}$	$\sigma_b^{\#}(T)(\text{MPa})$	$\sigma_b^{\#}(T)/\sigma_b$
20	180	1	1500	1	1703	1
300	175	0.97	1490	0.99	1705	1.00
400	185	1.03	1503	1.00	1731	1.02
500	173	0.96	1175	0.78	1306	0.77
600	171	0.95	929	0.62	961	0.56
700	190	1.06	485	0.32	683	0.40

Notes: T is the maximum exposure temperature, $E_s^{\#}(T)$ is the elastic modulus of steel wires after cooling from T , $\sigma_{0.2}^{\#}(T)$ is the nominal yield strength of steel wires after cooling from T , $\sigma_b^{\#}(T)$ is the ultimate strength of steel wires after cooling from T .

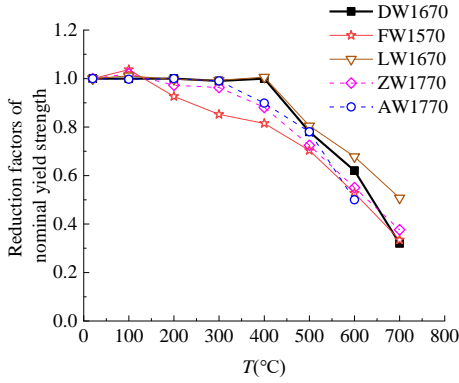


Fig. 18 Comparison of reduction factors of nominal yield strength

(2) Comparison of ultimate strength

As shown in Fig. 19, the reduction factors of FW1570 are visibly low. DW1670 is close to the others after cooling from temperatures below 300°C; close to LW1670 and higher than the others after exposure to 400°C. DW1670 is slightly lower than LW1670, close to AW1770, and slightly higher than ZW1770 after cooling from 500°C. When the maximum temperatures experienced by the specimens are above 600°C, DW1670 is close to ZW1770 and AW1770 and lower than LW1670.

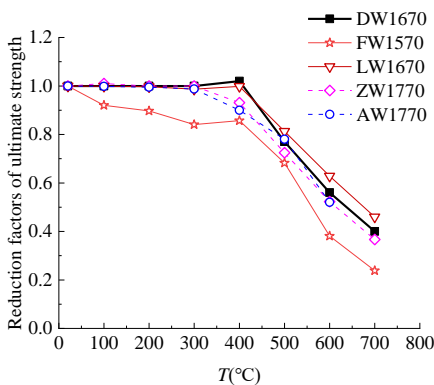


Fig. 19 Comparison of reduction factors of ultimate strength

In general, except for FW1570, the nominal yield strength and ultimate strength of different grades of steel wires begin to degrade significantly when the exposure temperature reaches above 400°C, and the decay trends are essentially consistent.

As can be seen in Fig. 18, the reduction factors of this paper (DW1670) are close to those of LW1670, ZW1770 and AW1770 after exposure to temperatures below 300°C; close to LW1670 and higher than others after cooling from 400°C. DW1670 is close to LW1670 and AW1770 and higher than ZW1770 and FW1570 after cooling from 500°C, and is only lower than LW1670 after exposure to 600°C. DW1670 decreases more quickly after cooling from 600°C and 700°C, and is obviously lower than LW1670 and close to the others after exposure to 700°C.

4.4. Fitting equation for reduction factors

According to the test data, fitting equations for reduction factors of mechanical properties of steel wires after exposed to elevated temperature are given as follows,

4.4.1. Elastic modulus

$$\frac{E_s^{\#}(T)}{E_s} = 1 \quad (8)$$

where, $E_s^{\#}(T)$ and E_s are the elastic modulus of the steel wire after cooling from temperature T and at ambient temperature, respectively.

4.4.2. Proportional limit

$$\frac{\sigma_p^{\#}(T)}{\sigma_p} = \begin{cases} 1 & 20^{\circ}\text{C} \leq T \leq 400^{\circ}\text{C} \\ -0.0019T + 1.7591 & 400^{\circ}\text{C} \leq T \leq 700^{\circ}\text{C} \end{cases} \quad (9)$$

where, $\sigma_p^{\#}(T)$ and σ_p are the proportional limit of the steel wire after cooling from temperature T and at ambient temperature, respectively.

The fitting curve of Eq. (9) is plotted in Fig. 20.

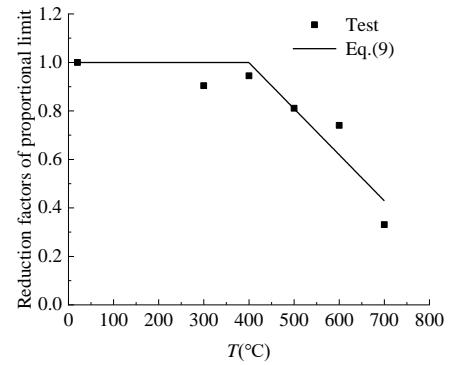


Fig. 20 Reduction factor of proportional limit-temperature curve

4.4.3. Ultimate strength

$$\frac{\sigma_b^{\#}(T)}{\sigma_b} = \begin{cases} 1 & 20^{\circ}\text{C} \leq T \leq 400^{\circ}\text{C} \\ -0.002T + 1.814 & 400^{\circ}\text{C} \leq T \leq 700^{\circ}\text{C} \end{cases} \quad (10)$$

where, $\sigma_b^{\#}(T)$ and σ_b are the ultimate strength of the steel wire after cooling from temperature T and at ambient temperature, respectively.

The fitting curve of Eq. (10) is shown in Fig. 21.

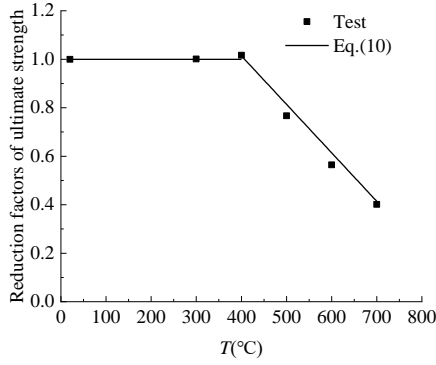


Fig. 21 Reduction factor of ultimate strength-temperature curve

4.4.4. Nominal yield strength

$$\frac{\sigma_{0.2}^{\#}(T)}{\sigma_{0.2}} = \begin{cases} 1 & 20^{\circ}\text{C} \leq T \leq 400^{\circ}\text{C} \\ -0.0022T + 1.892 & 400^{\circ}\text{C} \leq T \leq 700^{\circ}\text{C} \end{cases} \quad (11)$$

where, $\sigma_{0.2}^{\#}(T)$ and $\sigma_{0.2}$ are the nominal yield strength of the steel wire after cooling from temperature T and at ambient temperature, respectively.

Fig. 22 presents the fitting curve of Eq. (11).

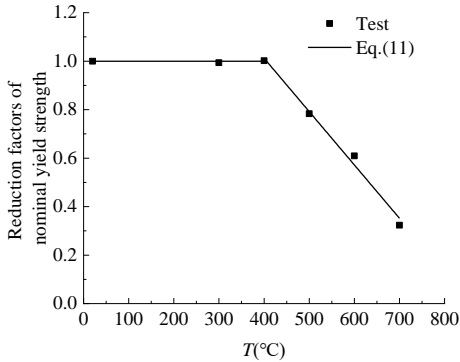


Fig. 22 Reduction factor of nominal yield strength-temperature curve

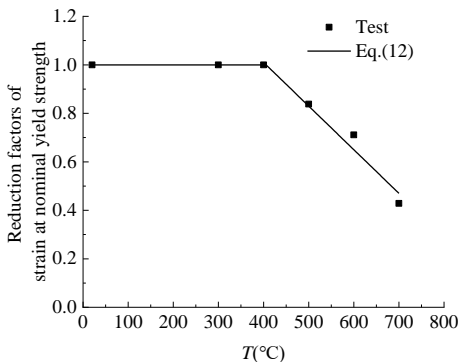


Fig. 23 Reduction factor of strain at nominal yield strength-temperature curve

4.4.5. Strain at nominal yield strength

$$\frac{\varepsilon_{0.2}^{\#}(T)}{\varepsilon_{0.2}} = \begin{cases} 1 & 20^{\circ}\text{C} \leq T \leq 400^{\circ}\text{C} \\ -0.0018T + 1.7591 & 400^{\circ}\text{C} \leq T \leq 700^{\circ}\text{C} \end{cases} \quad (12)$$

where, $\varepsilon_{0.2}^{\#}(T)$ and $\varepsilon_{0.2}$ are the strain at nominal yield strength of the steel wire after cooling from temperature T and at ambient temperature, respectively.

ly.

The fitting curve of Eq. (12) is plotted in Fig. 23.

4.5. Constitutive equation

By the same method as that at elevated temperatures, the constitutive equation of the steel wire after exposed to high temperatures is fitted with a trilinear line. The fitting equation is shown as follows,

$$\sigma = \begin{cases} E_s^{\#}(T) \times \varepsilon & 0 \leq \varepsilon \leq \frac{\sigma_p^{\#}(T)}{E_s^{\#}(T)} \\ \frac{\sigma_{0.2}^{\#}(T) - \sigma_p^{\#}(T)}{\varepsilon_{0.2}^{\#}(T) - \frac{\sigma_p^{\#}(T)}{E_s^{\#}(T)}} \times \left[\varepsilon - \frac{\sigma_p^{\#}(T)}{E_s^{\#}(T)} \right] + \sigma_p^{\#}(T) & \frac{\sigma_p^{\#}(T)}{E_s^{\#}(T)} \leq \varepsilon \leq \varepsilon_{0.2}^{\#}(T) \\ \frac{\sigma_b^{\#}(T) - \sigma_{0.2}^{\#}(T)}{\varepsilon_b^{\#}(T) - \varepsilon_{0.2}^{\#}(T)} \times \left[\varepsilon - \varepsilon_{0.2}^{\#}(T) \right] + \sigma_{0.2}^{\#}(T) & \varepsilon_{0.2}^{\#}(T) \leq \varepsilon \leq \varepsilon_b^{\#}(T) \end{cases} \quad (13)$$

Stress-strain curves of steel wires cooling from various temperatures obtained by the equation are exhibited in Fig. 24.

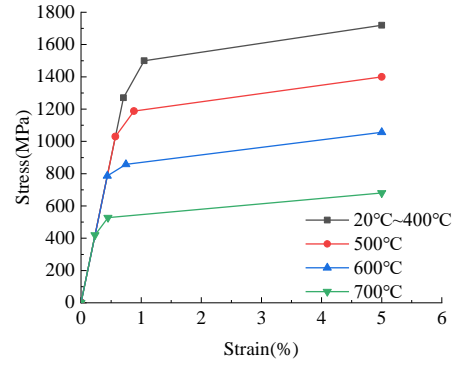


Fig. 24 Stress-strain fitting curves of steel wire after cooling from elevated temperatures

5. Conclusions

In this paper, elevated-temperature and post-elevated-temperature tensile tests were performed on Grade 1670 steel wires with a diameter of 7mm. The test results were compared with the existing test results of prestressed steel wires and steel cables. The following conclusions are obtained,

(1) At elevated temperatures, mechanical properties of the prestressed steel wire changed little with the temperature below 300°C and degraded significantly at 300°C ~ 600°C. The load-carrying ability was substantially lost when the temperature reached 700°C.

(2) After elevated temperatures, the elastic modulus of the steel wires had no obvious change with the exposure temperature. The nominal yield strength and ultimate strength of the steel wires remained unchanged after exposed to temperatures below 400°C, and tended to decrease after cooling from higher exposure temperatures.

(3) Equations of elevated-temperature and post-elevated-temperature mechanical behaviors of steel wires are fitted as a function of the temperature, and constitutive models of the steel wire at elevated temperatures and after exposed to elevated temperatures are obtained.

Acknowledgments

The research work described in this paper is sponsored by the Nation Natural Science Foundation of China (Grant No. 51808117). The financial support is highly appreciated.

References

- [1] Zhou H.T., Li G.Q. and Jiang S.C., "Experimental studies on the properties of steel strand at elevated temperatures", Journal of Sichuan University, 40(5), 106-110, 2008.
- [2] Zong Z.L., He Y.F. and Li S.G., "Analysis of the fire-resistance of prestressed steel structure based on mechanical properties of steel strands under the high temperature", Sichuan Building Science, 39(5), 47-51, 2013.
- [3] Zong Z.L., Zhang J., Jiang D.W. and Yao J.W., "Experimental research on the mechanical properties of steel strand wire at elevated temperature", Build Science, 32(1), 43-47, 2016.

- [4] Fontanari V., Benedetti M., Monelli B.D. and Degasperri F., "Fire behavior of steel wire ropes: Experimental investigation and numerical analysis", *Engineering Structures*, 84(1), 340-349, 2015.
- [5] Conon T., "Mechanical properties of cold-drawn steel strand at elevated temperatures", Lehigh University, 2015.
- [6] Shakya A.M. and Kodur V., "Effect of temperature on the mechanical properties of low relaxation seven-wire prestressing strand", *Construction and Building Materials*, 124(15), 74-84, 2016.
- [7] Du Y., Peng J.Z., Liew R. J.Y. and Li G.Q., "Mechanical properties of high tensile steel cables at elevated temperatures", *Construction and Building Materials*, 182(10), 52-65, 2018.
- [8] Du Y., Sun Y.K. and Li G.Q., "Mechanical properties of high tensile steel cables at elevated temperature", *Engineering Mechanics*, 36(4), 231-238, 2019.
- [9] Du Y., Qi H.H., Jiang J., Liew R. J.Y. and Li G.Q., "Mechanical properties of 1670MPa parallel wire strands at elevated temperatures", *Construction and Building Materials*, 263(8), 1-16, 2020.
- [10] Du Y., Xiao L.P., Li G.Q. and Wang X.C., "Mechanical properties of high tensile parallel wire cables at elevated temperatures", *Journal of Building Materials*, 23(1), 114-121, 2020.
- [11] Sun G.J., Li X.H. and Xue S.D., "Mechanical properties of stainless-steel cables at elevated temperature", *Journal of Materials in Civil Engineering*, 31(7), 1-10, 2019.
- [12] Sun G.J., Li X.H., Xue S.D. and Chen R.H., "Mechanical properties of Galfan-coated steel cables at elevated temperatures", *Journal of Constructional Steel Research*, 155(4), 331-341, 2019.
- [13] Sun G.J., Li Z.H., Wu J.Z. and Ren J.Y., "Investigation of steel wire mechanical behavior and collaborative mechanism under high temperature", *Journal of Constructional Steel Research*, 188(10), 1-14, 2022.
- [14] Fan J. and Lu Z.T., "Experimental study on materials properties of prestressed steel wire post high temperatures", *Industrial Building*, 32(9), 30-31, 2002.
- [15] Lu J., Liu H.B. and Chen Z.H., "Post-fire mechanical properties of low-relaxation hot-dip galvanized prestressed steel wires", *Journal of Constructional Steel Research*, 136, 110-127, 2017.
- [16] Lu J., Liu H.B. and Liu J.D., "Post-fire mechanical properties of Galfan-coated steel cables with extruded anchorages", *Journal of Tianjin University(Science and Technology)*, 50, 7-17, 2017.
- [17] Zheng W.Z., Hu Q. and Zhang H.Y., "Experimental research on the mechanical properties of prestressing steel wire at and after high temperature", *Journal of Building Structures*, 27(2), 120-128, 2006.
- [18] Atienza J.M. and Elices M., "Behavior of prestressing steels after a simulated fire: Fire-induced damages", *Construction and Building Materials*, 23(8), 2932-2940, 2009.
- [19] Zong Z.L., Zhang J., Jiang D.W. and Yao J.W., "Experimental research on the mechanical properties of steel strand after high temperature", *Fire Science and Technology*, 34(3), 311-314, 2015.
- [20] Zhang Z.L., Guo T., Wang S.Y., Liu J. and Wang L.B., "Experimental study on post-fire properties of steel wires of bridge suspender", *Structures*, 33(21), 1252-1262, 2021.
- [21] *Metallic materials-Tensile testing-Part 1: Method of test at room temperature (GB/T 228.1-2010)*, General Administration of Quality Supervision, Inspection and Quarantine of the People's Republic of China Beijing, China, 2010.
- [22] *Metallic materials-Tensile testing-Part 2: Method of test at elevated temperature (GB/T 228.2-2015)*, General Administration of Quality Supervision, Inspection and Quarantine of the People's Republic of China Beijing, China, 2015.